Adsorption and Photocatalysis Kinetics of Herbicide onto Titanium Oxide and Powdered Activated Carbon

Seoung-Hyun Kim, Huu Hao Ngo*, H. K. Shon, S. Vigneswaran

Faculty of Engineering, University of Technology, Sydney, P.O. Box 123, Broadway, NSW 2007, Australia

* Correspondence author, E-mail: Haon@uts.edu.au, Ph +612 9514 1693, Fax +612 9514 2633

ABSTRACT

The adsorption and photocatalysis kinetics of metsulfuron-methyl (MM) onto titanium oxide (TiO_2) and powdered activated carbon (PAC) were studied at varying adsorbent amount and MM concentration. The overall mass transfer in adsorption was estimated from concentration decay curves obtained in the batch adsorber. The maximum adsorption capacity decreased with increasing adsorbent amount in TiO_2 adsorption. The adsorption isotherms of MM could be plotted using the Langmuir isotherm model with a reasonable degree of accuracy having higher r^2 values rather than Freundlich isotherm model. Linear driving force approximation (LDFA) kinetic equation with Langmuir adsorption isotherm model was successfully applied to predict the adsorption kinetics data in various concentrations of MM in photobatch reactor. The estimated mass transfer coefficient was used to be 3.0×10^{-5}, 5.5×10^{-5}, 9.1×10^{-5} m/s in PAC adsorption and 2.0×10^{-5}, 1.1×10^{-5}, 9.0×10^{-6} m/s in TiO_2 adsorption for a different MM concentration of 20, 50 and 70 mg/L, respectively. Photocatalysis kinetics was same with TiO_2 of 0.2 g/L regardless of TiO_2 amounts and the MM degradation kinetics was enhanced by TiO_2 catalysis rather than only UV-light degradation. Among the photocatalysis kinetics model with first-order, second-order and Langmuir-Hinshelwood (L-H) model, a second-order kinetic model was found to well present the experimental data of MM by TiO_2 catalyst for the range of various TiO_2 amounts and MM concentration studied.

KEYWORDS: Photocatalysis, adsorption, Powdered activated carbon, Kinetics, Titanium oxide, Herbicide, Metsulfuron-methyl

1. INTRODUCTION

A major environmental concern at present is the contamination of aquatic systems due to pesticide discharges from manufacturing plants, surface runoff, leaching accidental spills, and other sources. Among the numerous agrochemicals in use today, the herbicide metsulfuron-methyl (MM) ($C_{14}H_{15}N_5O_6S$) is widely used to control broad-leaved weeds in the world. However, this compound may persist in the environment for many months. MM permeates into soil and subsequently run off from cropland into rivers and lakes, causing surface water pollution. Removal of these potentially harmful compounds from water has emerged as an important issue of environmental protection [1,2].

Titanium dioxide (TiO_2) catalyzed photocatalysis is broadly used because of its capability in removing a wide range of pollutants. The photochemical stability, low toxicity and low cost are the other advantages of TiO_2 [3-6]. It is well known that PAC can be very efficient when it is mixed with TiO_2 in photocatalytic processes [4]. Arana et al. observed that (i) the combination of PAC and TiO_2 resulted in fast decantability in comparison with that of TiO_2 alone, (ii) a TiO_2 particle distribution on the PAC surface yielded in a homogeneous particle size distribution, and (iii) the rate of organic removal by the PAC and TiO_2 was six times higher than that with TiO_2 alone [4]. A pretreatment of adsorption with powdered activated carbon (PAC) on photocatalysis showed that PAC adsorption followed by photocatalysis was not effective in alleviating reverse reaction. Here, the reverse reaction represents the increasing concentration with time during photocatlysis. On the other hand, when PAC and TiO_2 were added simultaneously, the reverse reaction was eliminated. Further, the organic removal was also improved by simultaneous PAC and TiO_2 additions [5]. Photocatalytic reactions allow in many cases a complete degradation of organic pollutants in very small and not noxious species, without using chemicals thus avoiding sludge production and its disposal. The process is based on the electronic excitation of a molecule or solid caused by light absorption ultraviolet (UV) light that drastically alters its ability to lose or gain electrons and promote decomposition of pollutants to harmless by-products [7-9]. Photoinduced electrons (e^-) and positive holes (h^+) are produced from TiO_2 with UV light (Equation 1). These charged species can further generate free radicals (Equations 2 and 3). The highly oxidizing positive hole h^+ has been considered to be the dominant oxidizing species contributing to the mineralization process resulting from the TiO_2 photocatalysis [10-12].

The combination of activated carbon adsorption and TiO_2 photocatalysis with microfiltration (MF)/ultrafiltration (UF) membranes is attractive as it takes advantages of both processes to treat the organics [13]. The fine activated carbons and TiO_2 particles should be separated from the treated water by membrane filtration and the optimum conditions should be found out in order to enhance the membrane permeate flux [14].

This work presents the adsorption of MM onto TiO_2 and PAC (powdered activated carbon). The objectives of this study are to investigate the adsorption characteristics and photocatalytic reaction of MM onto TiO_2 and PAC to obtain reliable information that will be applied in analyzing the MM adsorption and photocatalsis kinetics on TiO_2 and PAC.

2. EXPERIMENTAL

2.1. Materials

The photocatalyst, TiO_2, used in this study was Degussa P25 with surface area of 50 m^2/g, 6.9 nm mean pore size obtained from Degussa Company (Germany). Wood based powdered activated carbon (PAC) was also used from James Cumming & Sons Pty Ltd. (Australia). Tables 1 and 2 show the characteristics of TiO_2 and PAC used in this study. The commercial preparation of Metsulfuron-methyl (MM) group B herbicide (Australia Du Pont, 60 %, $C_{14}H_{15}N_5O_6S$) was used.

2.2 Adsorption equilibrium and batch test procedure

Adsorption equilibrium data were obtained by introducing predetermined weights of PAC and TiO_2 each 100 ml of mixed solution in Erlenmeyer flasks. MM solution of concentration ranging from 5 to 70 mg/L was used to get the adsorption equilibrium. Various TiO_2 amounts ranging from 0.2 to 3 g/L was added to the MM solution in Erlenmeyer flasks. A constant temperature incubator at 25 ºC for 48 hours was given sufficient contacting time for equilibrium.

After equilibrium was reached, a sample was taken from each flask. The concentrations of individual component were measured using an UV-Vis spectrophotometer (5625 Unicam Ltd., Cambridge, UK) in the range indicating a linear relationship between absorbance and concentration at 232 nm. The adsorbed amount (q) was calculated by following equation.

$$q = \frac{V(C_i - C_e)}{M} \quad (1)$$

Where q is the adsorbed amount (mg/g), V is the volume (L) of solution, C_i is the initial MM concentration (mg/L), C_e is the equilibrium MM concentration (mg/L), M is the amount of adsorbents (g).

Batch adsorption experiments were performed at 100 rpm with various TiO_2 amounts. Liquid samples were taken periodically by using an airtight precision syringe, withdrawing the solution from the reactor through the sample hole. The batch reactors were 1 L conical glass flask. In each flask, a known concentration of wastewater was mixed with the known amount of adsorbent ranging from 0.2 g/L to 3 g/L. All the experiments were carried out at a room temperature of 25 ºC and taken samples were filtered through 0.45 μm membrane prior to the concentration measurement.

2.3. Photocatalytic degradation

The photocatalysis experiment was conducted with powdered P25 Degussa TiO_2 particle as catalyst (Table 2). The photo reactor consisted of the three 8 watts UV light lamps, and mechanical stirrer (Figure 1). The surface area of the UV lamp was 141 cm^2. The volume of the reactor was 3 L and air sparging was provided to supply oxygen into the reactor (1.5 VVM). The circulation of tap water around the reactor controlled the temperature of the reactor at 25 °C.

3. RESULTS AND DISCUSSION

3.1. Adsorption equilibrium studies

In this study, Langmuir and Freundlich isotherm models were employed to destribe the MM adsorption equilibrium. The Langmuir isotherm is valid for monolayer adsorption onto a surface with a finite number of identical sites. It is given as Eq. (2):

$$q = \frac{q_m \cdot b \cdot C_e}{1 + b \cdot C_e} \quad (2)$$

The linearized form of the Langmuir equation is

$$\frac{C_e}{q} = \frac{1}{q_m \cdot b} + \frac{C_e}{q_m} \quad (3)$$

q_m and b can be determined from the linear plot of C_e / q versus C_e. The values q_m and b estimated from the plots along with the correlation coefficients are listed in Table 3. Langmuir isotherm model was reasonable to describing the MM adsorption equilibrium by TiO_2. The Langmuir constant q_m decreased with increasing adsorbent TiO_2 amount, while the variation of Langmuir constant b was not variable, indicating that adsorption density was higher at a lower adsorbent TiO_2 amount because of the limitation of TiO_2 adsorption capacity.

The Freundlich isotherm equation is given as below.

$$q = k \cdot C_e^{1/n} \quad (4)$$

k and n are the constants of adsorption density and adsorption intensity, respectively. Eq. (4) can be linearized as Eq. (5).

$$\ln q = \ln k + 1/n \cdot \ln C_e \quad (5)$$

The value of k and n can be estimated from the intercept and slope of the linear plot of experimental data of $\ln q$ versus $\ln C_e$. The Freundlich isotherm provides no information on the monolayer adsorption density in comparison with the Langmuir model.

The values of k and n from the linearized plots are shown in Table 3 following with the regression correlation coefficients. The parameter k related to the adsorption density increased with a decrease of adsorbent TiO_2 amount. The meaning of $n > 1.0$ indicates that MM was adsorbed favorable by TiO_2 at different adsorbent amounts. The regression correlation coefficients (r^2) model means that Freundlich isotherm model was slightly better for describing the adsorption equilibrium in a lower adsorbent part than Freundlich model, eventhough the Langmuir model also agreed with the experimental data well.

Figure 2 shows the equilibrium adsorption as a function of adsorbent TiO_2 amounts, with the increase of TiO_2 amount from 0.2 g/L to 3 g/L. At a lower TiO_2 amount, MM adsorption could reach higher adsorption capacity of all the conditions. At TiO_2 amount below 2.0 g/L, adsorption capacity significantly decreased with increasing TiO_2 amount. At a constant TiO_2 amount, the equilibrium adsorption capacity of MM increased with the increase in initial MM concentration

from 20 mg/L to 70 mg/L. Figure 3 indicates that MM adsorption equilibrium data by PAC without UV light were predicted by Freundlich and Langumir isotherm. Langmuir isotherm was good to fit data better than Freundlich isotherm.

3.2. Adsorption kinetic studies

The adsorption kinetics was described by linear driving force approximation (LDFA) model with total batch mass balance. It was selected because of its simplicity and use of MM concentration to represent the liquid phase concentration of the system. The material balance in the batch reactor can be described by [15-18].

$$\frac{dC}{dt} = -\frac{M}{V}\frac{dq}{dt} \tag{6}$$

The mass transfer rate between liquid and solid phases represented by the LDFA model, assuming that overall mass transfer coefficient unchanged during experiments is the following Eq. (7). [16-18].

$$\frac{dq}{dt} = \frac{3 \times k_f}{R \times \rho_p}\left(c_i - c_s\right) = k_m\left(q_s - q\right) \tag{7}$$

where R = radius of adsorbent (m), k_f =overall mass transfer coefficient (m/s), k_m =mass trans fer coefficient (1/s), c_i =MM fluid phase concentration (mg/L), c_s =equilibrium concentration (mg/L), q_s =adsorbed phase concentration at the external surface of adsorbent particle (mg/g), q =average adsorbed phase MM concentration (mg/g) and ρ_p =density of particle (kg/m^3). The adsorption rate of adsorbate by TiO_2 and PAC particle is linearly proportional to a driving force using the LDFA model, defined as the difference between the surface concentration and the average adsorbed-phase concentration. The values of k_f can be computed using the isotherm parameters and the above equations.

The adsorption kinetics of batch reactor with LDFA model was solved numerically by applying the orthogonal collocation method to discretize the equations. Discretization was done for the spatial variable, resulting in a set of time derivative ordinary differential equations (ODEs) for the adsorbate concentration. The resulting sets of ODEs were solved using Microsoft Developer Studio (Fortran Powder Station 4.0) by the subroutine LSODA [19-22].

Figure 4 shows the kinetics of adsorption at different initial concentrations of MM by TiO_2 and TiO_2 & PAC. The rate of adsorption was rapid in the initial minutes of solution–adsorbent contact and it reached the equilibrium state after 20 minutes. The amount of MM adsorbed increases with increase in the initial concentration. The estimated mass transfer coefficients used to predict the kinetic data were $3.0\times10^{-5,}$ 5.5×10^{-5}, 9.1×10^{-5} m/s in PAC adsorption and 2.0×10^{-5}, 1.1×10^{-5}, 9.0×10^{-6} m/s in TiO_2 adsorption for a different MM concentration. These experimental data were successfully predicted by LDFA kinetic equation with Langmuir adsorption isotherm model.

3.3. Photocatalysis kinetic studies

The photocatalytic degradation processes following the first-order, second-order and Langmuir-Hinshelwood kinetics are given by Equations (8), (9) and (10), respectively:

$$r = -\frac{dC}{dt} = k_1 \cdot C \tag{8}$$

$$r = -\frac{dC}{dt} = k_2 \cdot C^2 \tag{9}$$

$$r = -\frac{dC}{dt} = \frac{K_{ad} \cdot k \cdot C}{1 + K_{ad} \cdot C} \tag{10}$$

where r is the rate of MM concentration (hr^{-1} mg/L), C is the concentration at any time (mg/L), k_1 is the first-order rate constant (hr^{-1}), k_2 is the second-order rate constant (hr^{-1}), K_{ad} is the adsorption coefficient and k is the reaction rate constant. K_{ad} and k are the limiting rate constants of reaction at maximum coverage under the given experimental conditions and equilibrium constant for adsorption of MM onto TiO_2.

Integrating Equations (8) and (9) with respect to the limits $C = C_{ads}$ at time $t = 0$ and $C = C$ at time t, the non-linearized form of the first-order expression can be obtained as follows.

$$C = C_{ads} \cdot \exp^{-k_1 t} \tag{11}$$

$$C = \frac{C_{ads}}{k_2 \cdot C_{ads} t + 1} \tag{12}$$

where C_{ads} is concentration of solution at equilibrium without UV light (mg/L). The linearized Langmuir-Hinshelwood (L-H) expression can be given as follows.

$$\ln\frac{C}{C_{ads}} + K_{ad}\left(C_{ads} - C\right) = -K_{ad}\cdot k\cdot t \qquad (13)$$

where K_{ad} is the b of the Langmuir constant, and it is the apparent kinetic constant. The k value can be obtained by plotting $\ln C/C_{ads} + K_{ad}\left(C_{ads} - C\right)$ versus t [23]. Obtaining the K_{ad} values from nonlinear regression had a difficulty in assuming the initial value for K_{ad} [24]. The K_{ad} value should be obtained from adsorption equilibrium experiments in order to solve the above equation easily and could be calculated from Langmuir isotherm coefficient b.

Many researchers studied the L-H model kinetics to first-order by assuming the term $K_{ad}C << 1$. The L-H model kinetic expression can be as written in Equation (11) [24-27]. It means that Langmuir adsorption coefficient b is closer to 0 and initial concentration is very low. However, one has to find exact Langmuir adsorption coefficient b because concentration is not very low in this study. In case that physical adsorption is few effects to photocatalysis, one can ignore this physical adsorption effect. In this study, physical adsorption of MM on TiO_2 is a few effects to photocatalysis, which could not be ignored. In this manner, it is important that physical adsorption characteristics before the photocatalysis reaction on TiO_2 should be concerned to get the Lagnumir isotherm chefficient b exactly to get the photocatalysis kinetic values.

Figure 5 shows the experimental kinetic data depending on the only UV-light and the various TiO_2 amounts. It was reported about photodegradation that MM was degraded by UV light in aqueous solution [28]. Regardless of TiO_2 amounts, photocatalysis kinetics was similar to TiO_2 (0.2 g/L). The MM degradation kinetics was enhanced by TiO_2 catalysis rather than only UV-light degradation.

Figure 6 presents the adsorption and photocatalysis kinetics at different MM concentrations with TiO_2 and PAC. Non-linear method was used to estimate the parameters involved in the first-order, second-order and Langmuir-Hinshelwood (L-H) kinetic expression. All unknown parameters were obtained by non-linear method using Minpack program algorithm of Fortran Powerstation 4.0.

From Tables 4 and 5, it is observed that the first-order kinetics do not provide good fit to the experimental data for all initial MM concentrations. Of all other photocatalysis kinetics, the second-order kinetic expression with higher r^2 values was well fitted in terms of the phtocatalysis kinetics of MM degradation by TiO_2 catalyst. The lower r^2 value of L-H model and first-order kinetics model was inappropriate to represent the kinetics of photocatalysis of MM by TiO_2.

3.4. Changes of UV-Vis spectra

Figure 7 shows that the change of the optical densities of 232 nm of MM at different irradiation time under UV light. Absorption intensity of MM became weaker and weaker along with the irradiation time. This phenomenon indicated that MM molecules were attacked and removed under UV light and then produced a by-product at around 305 nm in absorption peak. Proposed pathway of degradation by UV light of MM was reported [28]. When PAC adsorption was used with TiO_2 photocatalysis, it improved the kinetics and removal efficiency without any by-product by PAC adsorption which can significantly remove the small molecular weight (Figure 8). Compared with TiO_2 photocatalysis UV-Vis spectra, TiO_2 photocatalysis and PAC adsorption system showed the better results. This can explain the improved photocatalysis activity of MM under UV light. The MM molecules and by-product have been introduced in PAC by adsorption process and TiO_2 by photocatalysis process, which could be useful system to remove herbicide in wastewater.

4. CONCLUSIONS

The adsorption and photocatalysis kinetics of MM onto TiO_2 and PAC were studied at varying adsorbent TiO_2 amount and MM concentration. Several conclusions made from this study are as follows:

- The adsorption isotherm data of MM on PAC and TiO_2 was fitted well with the Langmuir adsorption isotherm model.
- The rate of adsorption was rapid in the initial minutes of solution–adsorbent contact and it became equilibrium state after 20 minutes. The amount of MM adsorbed increases with

increasing in the initial concentration. It was successfully predicted under various concentrations of MM by LDFA kinetic equation with Langmuir adsorption isotherm model.

- Photodegradation of MM by only UV-light was degraded by UV light in aqueous solution. Regardless of TiO_2 amounts, photocatalysis kinetics was same with TiO_2 of 0.2 g/L and the MM degradation kinetics was enhanced by TiO_2 catalysis rather than only UV-light degradation.
- Among the photocatalysis kinetics model with first-order, second-order and Langmuir-Hinshelwood (L-H) model, a second-order kinetic model is found to well present the experimental data of MM by TiO_2 catalyst for the range of various TiO_2 amounts and MM concentration studied.
- PAC adsorption used in this experiment could improve the kinetics and removal efficiency. TiO_2 photocatalysis and PAC adsorption system could be explained as the MM molecules and by-product were removed efficiently in PAC by adsorption process and TiO_2 by photocatalysis process.

ACKNOWLEDGMENTS

This research was funded by the Korea Research Foundation by the Korean Government (MOEHRD) (KRF-2006-214-D00027) and UTS Chancellor's postdoctoral research fellow grant. The authors are also grateful to the supports from University of Technology (UTS) - Faculty of Engineering and Institute for Water and Environ mental Resource Management (IWERM).

REFERENCES

[1] Abdullah, A.R., Sinnakkannu, S., Tahir, N.M., Adsorption, desorption, and mobility of Metsulfuron Methyl in Malaysian agricultural soils, Bull. Environ. Conta. Toxicol. 66 (2001) 762-770.

[2] Celis R., Hermosin M.C., Carrizosa M.J., Cornejo J., Inorganic and organic clays as carriers for controlled release of the herbicide hexazione, J. Agric. Food Chem. 50 (2002) 2324-2330.

[3] Lianfeng Z., Tatsuo K., Noriaki S., Atsushi T., Development of TiO_2 photocatalyst reaction for water purification, Sep. Purif. Technol., 31(1) (2003) 105-110.

[4] Arana, J., Melian, J.A.H., Rodriguez, J.M.D., Diaz, O.G., Viera, A., Pena, J.P., Sosa, P.M.M., Jimenez, V.E., TiO_2-photocatalysis as a tertiary treatment of naturally treated wastewater. Catal. Today. 76 (2-4) (2002) 279-289.

[5] Shon H.K., Vigneswaran S., Ngo H.H., Kim J. H., Chemical coupling of photocatalysis with flocculation and adsorption in the removal of organic matter, Water Res. 39 (2005) 2549-2558.

[6] Areerachakul N., Vigneswaran S., Ngo H.H., Kandasamy J., Granular activated carbon (GAC) adsorption – photocatalysis hybrid system in the removal of herbicide from water, Sep. Purif. Technol. (2006) In press

[7] Molinari, R., Borgese M., Drioli E., Palmisano L., Schiavello M., Hybrid processes coupling photocatalysis and membranes for degradation of organic pollutants in water. Catal. Today 75 (1-4) (2002) 77-85.

[8] Gomes G. S., Joaquim L. F., Photochemical and photocatalytic degradation of an azo dye in aqueous solution by UV irradiation, J. Photoch. Photobio. A: Chemistry. 155(1-3) (2003) 133-143.

[9] Jianfeng F., Min J., Yaqian Z., Lizhang W., Kinetics of aqueous photocatalytic oxidation of fulvic acids in a photocatalysis–ultrafiltration reactor (PUR), Sep. Purif. Technol. 50(1) 69 (2006) 107-113.

[10] Qingzhong Y., Ravikrishna R., Valsaraj K. T., Reusable adsorbents for dilute solution separation. 5. Photodegradation of organic compounds on surfactant-modified titania, Sep. Purif. Technol., 24(1-2) (2001) 309-318.

[11] Gulten A., Mehmet A., Kadir Y., Removal of 2,4-dichlorophenoxyacetic acid from

aqueous solutions by partially characterized organophilic sepiolite: thermodynamic and kinetic calculations, J. Colloid Interf. Sci. 281 (2005) 27-32.

[12] Chu W., Wong C.C., The photocatalytic degradation of dicamba in TiO_2 suspensions with the help of hydrogen peroxide by different near UV irradiations, Water Res. 38(4) (2004) 1037-1043.

[13] Adham S.S., Snoeyink V.L., Clark M.M., Anselme C., Predicting and verifying TOC removal by PAC in pilot-scale UF systems, J. Am. Water Works Assoc. 85(12) (1993) 58-68.

[14] Yue J., Rong W., Anthony G. F., Atrazine adsorption from aqueous solution using powdered activated carbon-Improved mass transfer by air bubbling agitation, Chem. Eng. J. 116 (2006) 53-59.

[15] Misic, D. M., Sudo, Y., Suzuki, M., Kawazoe, K., Liquid to particle mass transfer in a stirred batch adsorption tank with nonlinear isotherm, J. Chem. Eng. Japan. 15 (1982) 67-70.

[16] Gordon M., Solution to the homogeneous surface diffusion model for batch adsorption systems using orthogonal collocation, Chem. Eng. J. 81(1-3) (2001) 213.

[17] Tien, C. Adsorption calculations and modelling. Butterworth-Heinemann, 1994.

[18] Chaudahry D.S., Vigneswaran S., Jegatheesan V., Ngo H.H., Shim W.G. and Kim S.H., Granular activated carbon adsorption in tertiary wastewater treatment; Experiments and models, Wat. Sci. Technol. 47(1) (2002) 113-120.

[19] Simone, C., Carlos, A. G. Alirio, E. R., Separation of Methane and Nitrogen by Adsorption on Carbon Molecular Sieve, Sep. Sci. Technol. 40 (2005) 2721-2743.

[20] Ouvrard S., Simonnot M.O., de Donato P. Sardin M. Diffusion-Controlled Adsorption of Arsenate on a Natural Manganese Oxide. Ind. Eng. Chem. Res. 41(24) (2002) 6194.

[21] Constales D., Kacur J., Computation and sensitivity analysis of the pricing of American call options, Appl. Math. Comput. 176(1) (2006) 302-307.

[22] LSODA subroutine, http://www.aei.mpg.de/~jthorn/teach/vienna.privatissimum/ode.html

[23] Chun-Hua L., Mei-Fang H., Shun-Gui Z., et al., The effect of erbium on the adsorption and photodegradation of orange I in aqueous Er^{3+}-TiO_2 suspension, J. Hazard. Mater., B138 (2006) 471–478.

[24] Vasanth K., Porkodi K., Selvaganapathi A., Constrain in solving Langmuir-Hinshelwood

kinetic expression for the photocatalysis degradation of Auramine O aqueous solutions by ZnO catalyst, Dyes Pigments, 1-4, (2006) In-press.

[25] Katsuyuki N., Eiko O., Shinsuke T., Ryuji Y., Teiji Tanizaki, Makoto T., et al., Photocatalytic treatment of water containing dinitrophenol and city water over TiO_2/SiO_2, Sep. Purif. Technol., 34(1-3) (2004) 67-72.

[26] Claudia G. S., Joaquim L.F., Photochemical and photocatalytic degradation of an azo dye in aqueous solution by UV irradiation. J. Photoch. Photobio. A: Chemistry, 155(1-3) (2003) 133-143.

[27] Saeed B. Bukallah, M.A. Rauf, Salman S. A., Photocatalytic decoloration of Coomassie Brilliant Blue with titanium oxide. Dyes and Pigments, 72(3) (2007) 353-356.

[28] Samanta S., Kole R.K., Chowdhury A., Photodegradation of metsulfuron methyl in aqueous solution, Chemosphere, 39(6) (1999) 873-879.

Table 1. Characteristics of photocatalyst TiO_2 used.

Specification	Degussa P25 TiO_2 photocatalyst
Structure	Non-porous
Components	65% anatase, 25% rutile, 0.2% SiO_2, 0.3% Al_2O_3, 0.3% HCl, 0.01% Fe_2O_3
Average aggregate particle diameter	Non-porous
Primary crystal size (μm)	3.0
Mean pore diameter (nm)	6.9
Band gap	3.03 (from 500 to 300 nm) with UV-Vis
Apparent density (kg/m^3)	130
Surface area (m^2/g)	42.32 ± 0.18
Type	Powdered
Product code	Degussa P25, Frankfurt am Main, Germany

Table 2. Characteristics of powdered activated carbon (PAC) used.

Specification	Powdered Activated Carbon (PAC)
Iodine number (mg/g min)	900
Ash content (%)	6 max.
Moisture content (%)	5 max.
Bulk density (kg/m^3)	290 ~ 390
Surface area (m^2/g)	882
Nominal size	80% min finer than 75 micron
Type	Wood based
Mean pore diameter (Å)	30.61
Micropore volume (cm^3/g)	0.34
Mean diameter (μm)	19.71
Product code	MD3545WB powder (James Cumming & Sons Pty Ltd., Australia)

Table 3. Adsorption isotherm parameters of MM on TiO_2 and PAC at 298.15 K

	Langmuir isotherm constants					
	PAC 0.2 g/L	TiO_2 3 g/L	TiO_2 2 g/L	TiO_2 1 g/L	TiO_2 0.5 g/L	TiO_2 0.2 g/L
q_m	339.60	21.40	19.060	30.570	51.310	114.20
b	0.51	0.010	0.017	0.020	0.015	0.008
r^2	0.999	0.983	0.990	0.991	0.994	0.985
	Freundlich isotherm constants					
	PAC 0.2 g/L	TiO_2 3 g/L	TiO_2 2 g/L	TiO_2 1 g/L	TiO_2 0.5 g/L	TiO_2 0.2 g/L
k	207.10	0.346	0.573	1.241	1.445	1.534
n	8.75	1.281	1.428	1.542	1.425	1.272
r^2	0.985	0.981	0.988	0.996	0.997	0.992

Table 4. Photocatalysis kinetics parameters of MM in terms of TiO_2 amounts.

(Temp. = 298.15 K, MM=30 mg/L, Reactor volume = 3L, 8 watts UV light 3 lamps)

Condition	k_1 (hr^{-1})	r^2	k_2	r^2	k	K_{ad}	r^2
Only UV-light	0.118	0.901	0.006	0.956			
0.2 g/L	0.124	0.936	0.011	0.985	0.008	13.63	0.957
0.5 g/L	0.143	0.788	0.011	0.880	0.015	5.832	0.853
1g/L	0.142	0.909	0.010	0.959	0.020	4.289	0.910
2 g/L	0.125	0.908	0.009	0.965	0.017	4.959	0.880

Table 5. Photocatalysis kinetics parameters of MM in terms of MM concentrations.

(Temp. = 298.15 K, Reactor volume = 3L, TiO_2 = 0.2 g/L, 8 watts UV light 3 lamps)

Co (mg/L)	k_1 (hr^{-1})	r^2	k_2	r^2	k	K_{ad}	r^2
20	0.217	0.645	0.026	0.872	18.960	0.008	0.942
50	0.099	0.911	0.003	0.953	12.45	0.008	0.905
70	0.140	0.880	0.003	0.934	9.984	0.008	0.937

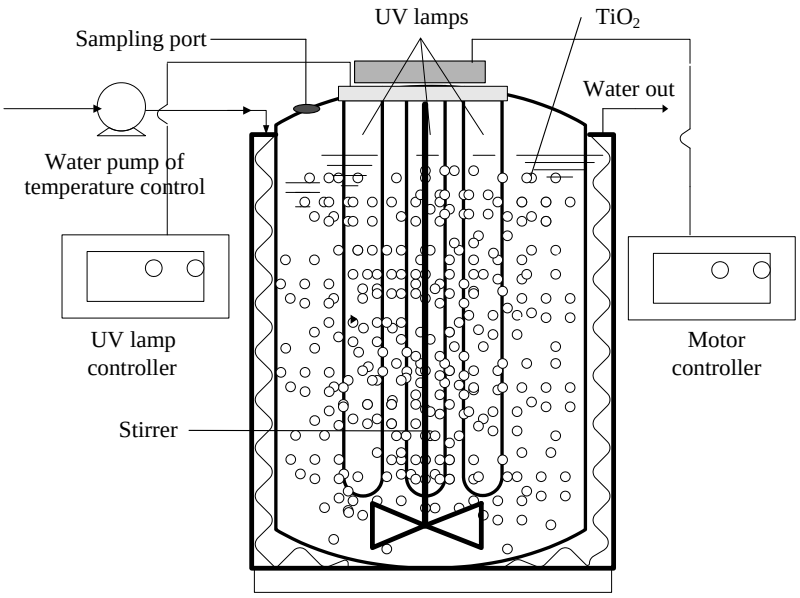

Figure 1. Schematic diagram of the photocatalytic batch reactor.

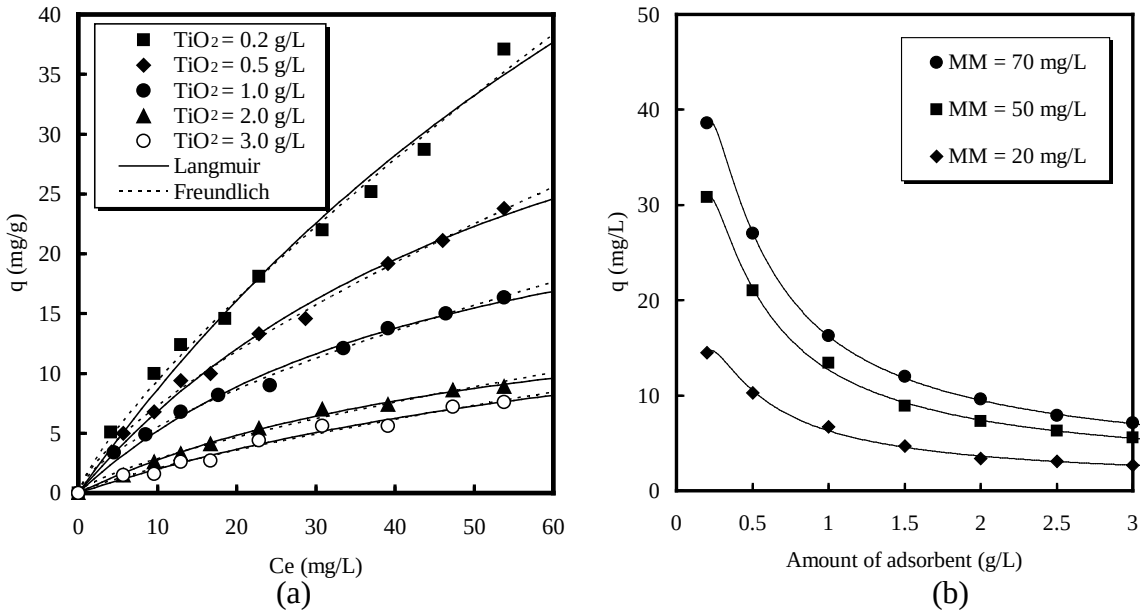

Figure 2. Effect of TiO_2 amount and initial MM concentration in adsorption equilibrium, (a) adsorption isotherm amount depending on TiO_2 amount, (b) adsorption amount depending on initial MM concentrations without UV light. (Temp.=298.15 K, Reactor volume= 0.1 L)

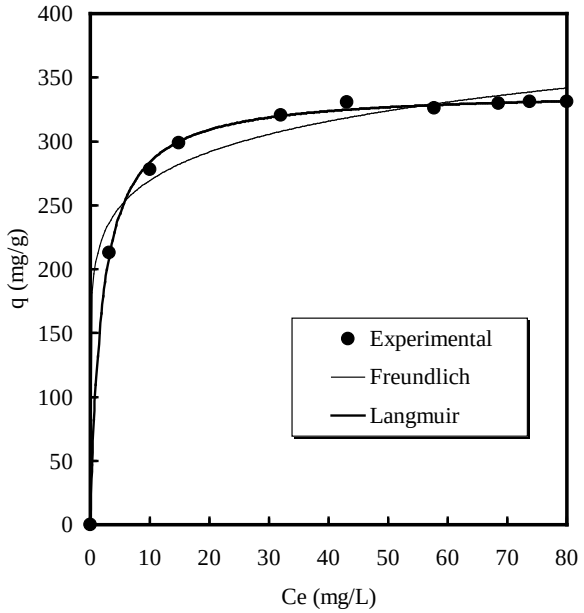

Figure 3. Adsorption isotherm of MM by PAC without UV light.
(Temp.=298.15 K, Reactor volume= 0.1 L)

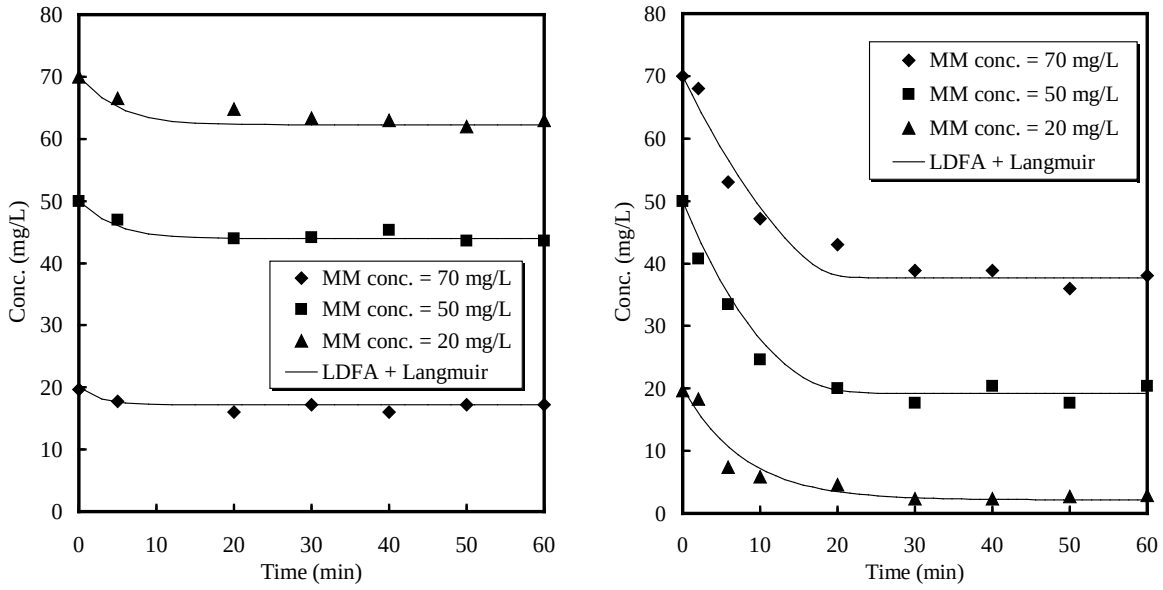

Figure 4. Kinetic experiments with different MM concentration. (a) TiO_2 adsorption kinetics experiments without UV-light, (b) PAC adsorption kinetics experiments without UV-light. (TiO_2 = 0.2 g/L, PAC=0.1 g/L, Reactor volume =3 L)

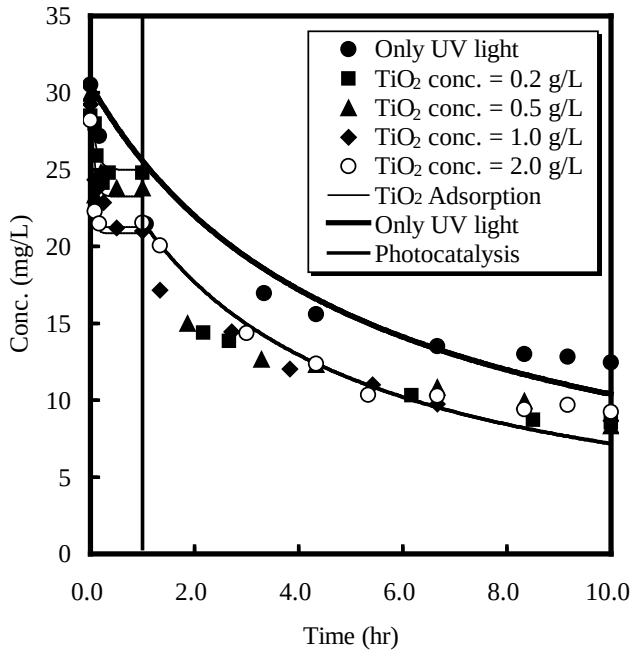

Figure 5. Effect of adsorption kinetics without UV-light, only UV light photodegradation and TiO_2 photocatalysis degradation in terms of various TiO_2 amount. (MM=30 mg/L, Reactor volume = 3L, 8 watts UV light 3 lamps)

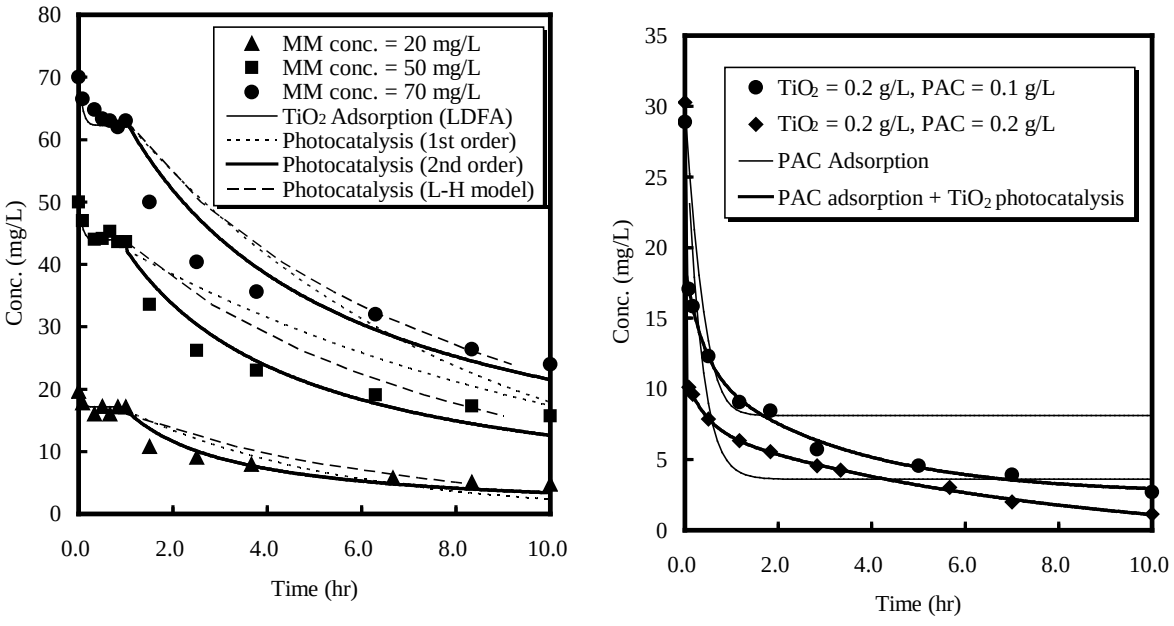

Figure 6. Comparison of various kinetics models. (a) Photocatalysis kinetics model after TiO_2 adsorption without UV light in terms of different initial MM concentrations, (b) PAC adsorption and TiO_2 photocatalysis kinetics onto TiO_2 and PAC. (Reactor volume = 3 L, 8 watts UV light 3 lamps)

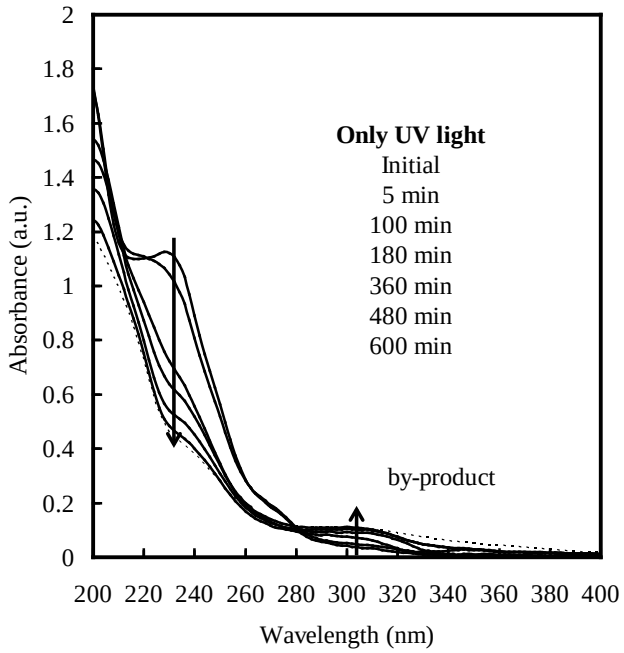

Figure 7. The change of UV-Vis absorption spectra of MM under only UV light (MM conc. = 30 mg/L, Reactor volume = 3L, 8 watts UV light 3 lamps)

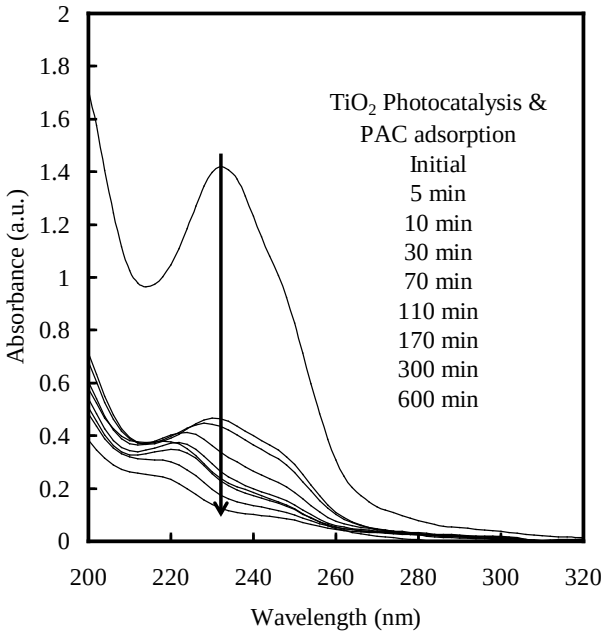

Figure 8. The change of UV-Vis spectra absorption spectra of MM under UV light (MM conc. = 30 mg/L, PAC = 0.2 g/L, TiO_2 = 0.2 g/L, 8 watts UV light 3 lamps).

LIST OF TABLES

LIST OF FIGURES